Impact of cavity on interatomic Coulombic decay

Lorenz S. Cederbaum* and Alexander I. Kuleff†

Theoretische Chemie, Physikalisch-Chemisches Institut, Universität Heidelberg, Im Neuenheimer Feld 229, Heidelberg D-69120, Germany

(Dated: December 30, 2020)

Abstract

The impact of quantum light on interatomic Coulombic decay (ICD) is investigated. In ICD the excess energy of an excited atom A is efficiently utilized to ionize a neighboring atom B. In quantum light an ensemble of atoms A form polaritonic states which can undergo ICD with B. It is shown that this process is dramatically altered compared to classical ICD. The ICD rate depends sensitively on the atomic distribution and orientation of the ensemble. General consequences are discussed.

* E-mail: Lorenz.Cederbaum@pci.uni-heidelberg.de

† E-mail: Alexander.Kuleff@pci.uni-heidelberg.de

Research Square

Preprints are preliminary reports that have not undergone peer review. They should not be considered conclusive, used to inform clinical practice, or referenced by the media as validated information.

Interatomic or intermolecular Coulombic decay (ICD) is a nonlocal and efficient electronic decay mechanism taking place in weakly bound matter. ICD becomes operative once the excess energy of an excited atom or molecule suffices to ionize a neighbor [1]. The energy released by the electronic relaxation of this excited atom or molecule ionizes the neighbor and hence energy conservation is fulfilled without the need for nuclear motion. As a consequence, the excited species as well as the neighbors can be atoms or molecules and the timescale involved is typically in the femtosecond regime [2–4]. Being ultrafast, ICD quenches in most cases concurrent electronic and nuclear mechanisms [5–8]. ICD has a wide range of applications. It has been shown to be active in the quantum halo systems He_2 [9, 10] and LiHe [11] where the mean separation of the atoms is extreme, in quantum dots and quantum wells [12–15], and its potential importance in radiation damage and for biologically relevant systems has also been discussed [5, 6, 16–20]. A recent review covers the fundamental and applied aspects of ICD and related processes [21].

The interaction of atoms and molecules with quantized radiation field like that inside a cavity has lead to an active new area of research which opens up many possibilities to manipulate their properties, to enhance or suppress available mechanisms, and to mediate new ones. Among the long list of possibilities we mention control of photochemical reactivity [22, 23] control of chemical reactions by varying the properties of the quantized field [24–27], enhance charge [28–31] and energy transfer [30, 32] processes, and increase non-adiabatic effects in molecules [26, 33, 34]. It is known that a classical laser field can induce a conical intersection even in a single diatomic molecule [35–37]. Indeed, a quantized radiation field also induces a conical intersection in a diatomic with new implications on its dynamic properties [38–40] and, of course, also in polyatomics [40, 41]. New types of intersections appear when more molecules are subject to the same quantized field where the molecules interact with each other via the field. Here, we mention the collective conical intersection which gives rise to unusual dynamics [42].

The main aim of the present work is to demonstrate and discuss the substantial impact the interaction with quantized light exerts on ICD. To be specific, we concentrate on atoms. Due to the interaction with the cavity mode, mixed electronic-photonic (polaritonic) state are formed [43]. In polaritonic states the atoms are entangled and one can expect interference effects to play a role. Constructive interference effects have been shown to enhance resonant photoionization in a multiatom ensemble [44]. A cavity is a particularly suitable platform

to investigate ICD as the entanglement is naturally produced in the polaritonic states.

We consider an ensemble of N non-interacting identical atoms of the kind A in a cavity with a quantized light mode (cavity mode) of frequency ω_c and polarization direction $\vec{\epsilon}_c$. The total Hamiltonian of the ensemble-cavity system reads [43, 45–47]:

$$H = H_e + \hbar\omega_c \hat{a}^\dagger \hat{a} + g\vec{\epsilon}_c \cdot \vec{d}(\hat{a}^\dagger + \hat{a}), \tag{1}$$

where $H_e = \sum_{i=1}^{N} H_i$ is the electronic Hamiltonian of the ensemble, $\vec{d} = \sum_{i=1}^{N} \vec{d}_i$ is the total dipole operator of the ensemble and g is the coupling strength between the cavity and the atoms. The quadratic dipole self-energy term is neglected as it is only of relevance for very strong coupling.

Since all atoms are of the same kind and we assume the cavity mode to be resonant with an excited atom A^*, it is straightforward to find the energies and eigenstates of the above Hamiltonian in the single-excitation space. For that purpose we define the contributing space to be spanned by $\{A_1 A_2 ... A_N 1_c\}$, which is the configuration state of the ensemble in its electronic ground state and the cavity in a single photon state, and the N configuration sates $\{A_1 ... A_i^* ... A_N 0_c\}$, $i = 1, ..., N$, where one atom is excited and the remaining $N-1$ are in their electronic ground state and the cavity has zero photons. Representing the Hamiltonian (1) in a single-excitation space, generally leads to an arrowhead matrix the properties of which have been analyzed in various contexts [48–50]. In the present case the matrix is particularly simple and can be solved in closed form.

It is well known that one obtains two so called bright states and $N-1$ dark states. Choosing the energy of A in its ground electronic state to be the origin of the energy scale, the bright states have the energies $\hbar\omega_c \pm \sqrt{N}g$ and the dark states are degenerate with energy $\hbar\omega_c$. The eigenstates of the former are

$$\Phi_{up/lp} = \frac{1}{\sqrt{2}} \left[\{A_1 ... A_N 1_c\} \pm \frac{1}{\sqrt{N}} \sum_{n=1}^{N} \{A_1 ... A_i^* ... A_N 0_c\} \right] \tag{2}$$

and seen to be superpositions of electronic states with one cavity photon and electronic states without cavity photon and are labeled upper and lower polariton states. One of the dark states takes on the appearance

$$\Phi_d = \frac{1}{\sqrt{N}} \sum_{n=1}^{N} (-1)^i \{A_1 ... A_i^* ... A_N 0_c\}, \tag{3}$$

where, for simplicity of presentation, we have chosen N to be even. Then, $\sum_{n=1}^{N}(-1)^i = 0$, and the other dark states can be obtained by permuting the $N/2$ minus signs such that the $N-1$ dark states are orthogonal to each other. The dark states do not contain configurations with cavity photons and the effect of the cavity is to create 'traceless' superpositions of the zero photon configurations. To better understand the notion of dark and bright, one notices that the transition matrix element with any one-atom operator $\hat{O} = \sum_{n=1}^{N} \hat{o}_i$ between the ground state $\Phi_0 = \{A_1 A_2 ... A_N 0_c\}$ of the ensemble-cavity system and a dark state vanishes: $\langle \Phi_0 | \hat{O} | \Phi_d \rangle = 0$. In contrast, the transition moment of a polariton state takes on the value $|\langle \Phi_0 | \hat{O} | \Phi_{up/lp} \rangle|^2 = N |\langle A | \hat{o} | A^* \rangle|^2 / 2$ as if all the available transition moments of all atoms is shared by the two polariton states. Since the coupling of the atoms to an external laser field is by an one-atom operator, the dark states are not populated by the laser while the polariton states are efficiently populated. The fact that the energies of the latter are separated from the former is favorable for populating the polariton states.

We now introduce a foreign atom B which we name impurity into the cavity. Before discussing the ICD in the cavity, we first consider the known situation of a single atom A and a neighbor B in the absence of a cavity. For ICD to be operative the excitation energy E_A of A must exceed the ionization potential of B (IP_B). Then, we have

$$A^* \cdots B \rightarrow A \cdots B^+ + e_{_{ICD}}, \tag{4}$$

where $e_{_{ICD}}$ stands for the electron emitted by ICD, briefly, the ICD electron. The kinetic energy of this electron is $E_A - IP_B$. At large interatomic distance R between A and B and dipole allowed transition $A^* \rightarrow A$, the ICD rate takes on the appearance $\Gamma = 2\pi |\gamma / R^3|^2$, where the decay amplitude γ can be expressed as the sum of products of amplitudes describing processes on the individual atoms, i.e., the deexcitation of atom A and the ionization of atom B [51, 52]. For closed-shell atoms A and B, one finds

$$\gamma = \vec{D}_A \cdot \vec{D}_B - 3(\vec{D}_A \cdot \vec{u})(\vec{D}_B \cdot \vec{u}), \tag{5}$$

where $\vec{u}$ is the unit vector pointing from B to A, $\vec{D}_A = \langle A^* | \vec{d}_A | A \rangle$ is the dipole transition matrix element for the deexcitation of A and $\vec{D}_B = \langle B | \vec{d}_B | B^+ \rangle$ is that for the ionization of B. Here, $|B\rangle$ is the initial state of B before ICD took place, $|B^+\rangle$ is the ion including the emitted electron produced by ICD, and $\vec{d}_{A(B)}$ are the dipole operators of $A(B)$.

It is relevant to note that the transition driven by the dipoles parallel to the interatomic axis (σ transition) gives rise to a decay amplitude which is twice as large as that driven

by the dipoles perpendicular to this axis (π transition), i.e., $\gamma_\sigma = -2\gamma_\pi$, and, consequently, the respective ICD rates fulfill $\Gamma_\sigma = 4\Gamma_\pi$ [51]. This phenomenon is counterintuitive at first sight, as it holds at large separations where the atoms are expected to be independent of each other.

We return to the ensemble of atoms A and the cavity. For that purpose we set the atom B at the origin of a coordinate system, choose the polarization direction $\vec{\epsilon}_c$ of the cavity as the Z-axis, and assign an index i to the unit vector $\vec{u}_i$ pointing from B to the i-th atom A_i of the ensemble. The situation is depicted in Fig. 1. Employing spherical coordinates, each unit Cartesian vector becomes as usual $\vec{u}_i = (\cos(\phi_i)\sin(\theta_i), \sin(\phi_i)\sin(\theta_i), \cos(\theta_i))$. Due to the cavity, the dipole transition elements $\vec{D}_{A_i}$ of all atoms A point parallel to the Z-axis and having the same absolute value can be written as $\vec{D}_{A_i} = D_A(0,0,1)$. To proceed, we construct for each atom pair A_i-B the decomposition of $\vec{D}_{A_i}$ into its components parallel and perpendicular to the respective unit vector:

$$\begin{aligned}\vec{D}^{\parallel}_{A_i} &= D_A\cos(\theta_i)(\cos(\phi_i)\sin(\theta_i), \sin(\phi_i)\sin(\theta_i), \cos(\theta_i)),\\ \vec{D}^{\perp}_{A_i} &= D_A\sin(\theta_i)(-\cos(\phi_i)\cos(\theta_i), -\sin(\phi_i)\cos(\theta_i), \sin(\theta_i)).\end{aligned} \tag{6}$$

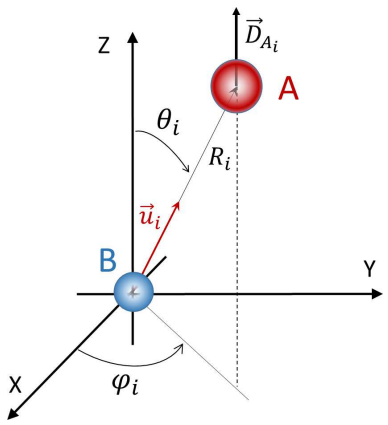

FIG. 1. Coordinate system and vectors used. The atom B is at the origin and its distance to an atom A_i of the ensemble is R_i. The unit vector $\vec{u}_i$ points from B to A_i and its spherical coordinates are θ_i and ϕ_i. The transition dipole $\vec{D}_{A_i}$ of A_i is parallel to the Z-axis and the polarization axis of the cavity.

Now we are in the position to compute the ICD rate of the ensemble in the cavity. As

done for a single pair of atoms, one starts from the golden rule

$$\Gamma = 2\pi \sum_f |\langle \Psi_i | V | \Psi_f \rangle|^2, \tag{7}$$

where V is the interaction between the atoms A and the impurity B. The wavefunctions Ψ_i and Ψ_f describe as usual the initial and final states of the process in the absence of this interaction. For a single pair, the initial state is given by the product $\Psi_i = \{A^*\}\{B\}$ and the final state by $\Psi_f = \{A\}\{B^+\}$, and the golden rule has lead to the rate $\Gamma = 2\pi|\gamma/R^3|^2$ with the amplitude γ presented in Eq. (5) [21, 51]. For the ensemble in the cavity the initial and final wavefunctions take on the appearance $\Psi_i = \Phi_{up/lp}\{B\}$ and $\Psi_f = \Phi_0\{B^+\}$ and analogously for the dark states. In complete analogy to the pair of atoms, the golden rule leads to the following relations for the polariton states

$$\begin{aligned} \Gamma &= \frac{2\pi}{2N} \left| \sum_{i=1}^{N} \gamma_i / R_i^3 \right|^2 , \\ \gamma_i &= \vec{D}_{A_i}^{\parallel} \cdot \vec{D}_B - 3D_A \cos(\theta_i) \vec{D}_B \cdot \vec{u}_i + \vec{D}_{A_i}^{\perp} \cdot \vec{D}_B, \end{aligned} \tag{8}$$

where R_i is the interatomic distance between atom A_i of the ensemble and B.

Since $\vec{D}_B$ is a vector, it is useful to first investigate the relevant quantity $\sum_{i=1}^{N} \gamma_i / R_i^3$ in the above equation separately for its three basis vectors in X, Y and Z directions, which we just call S_X, S_Y and S_Z. Choosing $\vec{D}_B = D_B(0,0,1) = D_B \vec{e}_Z$, and similarly for the other directions, leads with the aid of the explicit expressions in Eq. (6) to

$$\begin{aligned} S_Z &= -\gamma_\pi \sum_{i=1}^{N} \left[\frac{3\cos^2(\theta_i) - 1}{R_i^3} \right], \\ S_X &= -\frac{3\gamma_\pi}{2} \sum_{i=1}^{N} \left[\frac{\sin(2\theta_i)\cos(\phi_i)}{R_i^3} \right], \\ S_Y &= -\frac{3\gamma_\pi}{2} \sum_{i=1}^{N} \left[\frac{\sin(2\theta_i)\sin(\phi_i)}{R_i^3} \right]. \end{aligned} \tag{9}$$

Z is the polarization direction of the cavity and S_Z is seen to depend only on the θ_i angles of the atoms of the ensemble. Notice that γ_π is the decay amplitude of a single pair in the absence of the cavity.

The final transition matrix element for the ionization of B and with it the decay rate can

be written as

$$\vec{D}_B = D_B \left[S_X \vec{e}_X + S_Y \vec{e}_Y + S_Z \vec{e}_Z \right] / C,$$
$$\Gamma = \frac{2\pi}{2N} \left[|S_X|^2 + |S_Y|^2 + |S_Z|^2 \right], \tag{10}$$

where $C = 1/\left[|S_X|^2 + |S_Y|^2 + |S_Z|^2 \right]^{1/2}$ is a normalization constant.

From the above equations it can already be anticipated that the ICD process in a cavity is highly sensitive to the geometrical arrangement of the atoms of the ensemble. We shall also see that the location of the impurity with respect to the atoms of the ensemble plays a crucial role in the ICD process and this well beyond the trivial fact that ICD depends on the distance between the atoms of the ensemble and the impurity. Let us start the discussion by putting the ensemble and the impurity in the plane perpendicular to the polarization direction of the cavity. In this simple scenario, all θ_i angles are $\pi/2$ and $S_X = S_Y = 0$ and the ICD rate is

$$\Gamma = \frac{\Gamma_\pi}{2N} \left| \sum_{i=1}^{N} (R/R_i)^3 \right|^2, \tag{11}$$

where Γ_π is the ICD rate of a single pair at distance R in the absence of cavity. Clearly, the ICD rate of the ensemble in the cavity depends only on the distribution of the distances between the A atoms and the impurity. In general, the atoms which are close to the impurity contribute most to the rate, and because of the $2N$ denominator, the ICD rate is expected to be small for large numbers N of atoms. That entanglement can stabilize the ensemble against ICD can also be nicely observed for an ordered ensemble. Consider a linear chain of N atoms A lying in the XY-plane with interatomic distance R between adjacent atoms and the central atom is replaced by the impurity B. It is easy to evaluate the rate with the above equation. For $N = 2$, i.e., one A atom on each side of B, the rate is $\Gamma = 2\Gamma_\pi$ and thus twice as large as that without the cavity, but the situation changes as N grows. For large enough N one obtains $\Gamma = 2.88\,\Gamma_\pi/N$ which can be rather small for large N.

The situation changes dramatically when the atoms A form a ring around B. Then, all atoms A_i have the same distance R from the impurity and the ICD rate of a polariton state grows linearly with N:

$$\Gamma = \Gamma_\pi N/2. \tag{12}$$

Each of the polariton states shares half of the maximally possible decay rate where each A atom contributes Γ_π to the decay. As a consequence one notes that a dark state of the

ring ensemble cannot decay by ICD and its decay rate vanishes. This also follows from the golden rule, Eq. (7), using $\Psi_i = \Phi_d\{B\}$.

We continue with the ring ensemble and shift the impurity vertically out of the center of the ring, see Fig. 2b. Again, all atoms of the ensemble have the same angle θ, but this angle depends on the distance of the impurity B from the center of the ring. Consequently, in general S_X and S_Y do not vanish unless the atoms of the ensemble are equidistantly located on the ring. In this equidistant case, the rate follows, see Eqs. (8,9), a particularly simple expression

$$\Gamma = \frac{\Gamma_\pi N}{2}\left[3\cos^2(\theta) - 1\right]^2, \tag{13}$$

where Γ_π is the rate of a single pair undergoing ICD without the cavity. It is seen that due the entanglement of the ensemble's atoms there is an explicit dependence of the rate on the second Legendre polynomial in θ. This causes the rate to disappear at the magic angle $\theta = 54.74°$. Magic angles appear in many areas of physics like in photoionization [53] and NMR [54]. In the present context, the ring becomes stable against decay by ICD at the magic angle.

Next, we depart from the ensemble being confined to a plane perpendicular to the polarization direction of the cavity by tilting the ring with B in its center. To be specific the ring is rotated around the Y-axis by an angle χ, see Fig. 2. Then, each point $(\cos(\phi_{pi}), \sin(\phi_{pi}), 0)$ on the planar ring becomes $(\cos(\chi)\cos(\phi_{pi}), \sin(\phi_{pi}), \sin(\chi)\cos(\phi_{pi}))$ which determines the θ_i, ϕ_i angles needed to compute the ICD rates via Eqs. (9,10) of the tilted ring. This leads to

$$\begin{aligned}
S_X &= -\frac{3N\cdot\gamma_\pi}{4R^3}\sin^2(2\chi), \qquad S_Y = 0,\\
S_Z &= -\frac{N\gamma_\pi}{R^3}\left[3\sin^2(\chi)/2 - 1\right],\\
\Gamma &= \frac{N\Gamma_\pi}{2}\left[\frac{9}{16}\sin^4(2\chi) + \left(\frac{3}{2}\sin^2(\chi) - 1\right)^2\right].
\end{aligned} \tag{14}$$

In the derivation of the above equation it has been assumed that the atoms of the ensemble are distributed equidistantly on the ring. If this is not the case, the expressions become more involved and show that the ICD decay reflects the distribution on the ring.

At zero tilt ($\chi = 0$), the transition dipole $\vec{D}_B$ of the impurity points along the polarization axis of the quantized light and the decay rate is $N\Gamma_\pi/2$. Tilting the ring now makes this dipole rotate into the XZ-plane. Once the tilt arrives at the magic tilt angle ($\chi = 54.74°$), the

dipole in the polarization direction vanishes and now points completely in the X-direction and the rate becomes $2N\Gamma_\pi/9$. We mention here that not only the rate is a measurable quantity, but also the angular distribution of the emitted ICD electron is measurable, see, e.g., [55, 56], and this distribution depends on the direction of the transition dipole.

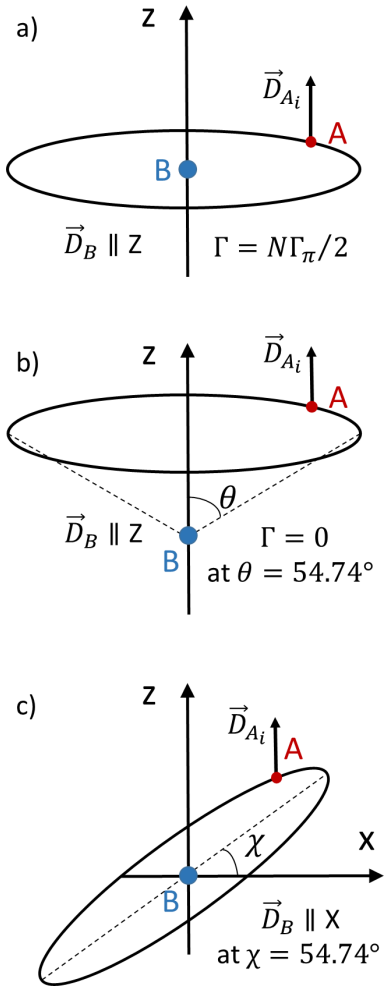

FIG. 2. The atoms A_i on a ring. a) The ring is in the XY-plane with B in the center. The ICD rate is strongly enhanced in the cavity from Γ_π without a cavity to $N\Gamma_\pi/2$. b) The ring is shifted along Z. The ICD rate now depends on the angle θ, see Eq. (13). There is no ICD at all at the magic angle. c) B is in the center and the ring is rotated around the Y-axis. The transition dipole of B rotates from the Z-axis into the XZ-plane and the ICD rate depends on the tilt angle, see Eq. (14). At the magic tilt angle, the transition dipole points parallel to the X-axis

Atomic and molecular clusters have been subject to continuous interest over many years [57, 58] and much interest has been devoted to their possible ground state geometrical

structures and properties. Many ICD experiments have been carried out with rare gas clusters [21] and as the interaction of the atoms is weak this makes them particularly suitable for cavity investigations. We consider here $ArNe_{12}$ as an example. Several energetically low-lying stable local structure are obtained by optimization with an universal force field [59]. The highest in symmetry is an icosahedral structure with a Ne-Ar distance $R = 3.406$ Å, see Fig. 3a. Without a cavity, a weak external laser would excite a single Ne atom which undergoes ICD with the central Ar atom. For $2p \rightarrow 3s$ transition, the ICD rate Γ_π corresponds to a ICD lifetime of 375 fs which is nearly 4 orders of magnitude shorter than the radiative lifetime of 1.6 ns [52]. Putting the $ArNe_{12}$ cluster in the cavity with the highest symmetry axis along Z (4 Ne atoms in each XY, XZ and YZ plane) and employing Eqs. (9,10) has surprised us considerably. The result is $\Gamma = 0$. That is, the cluster is stable against ICD.

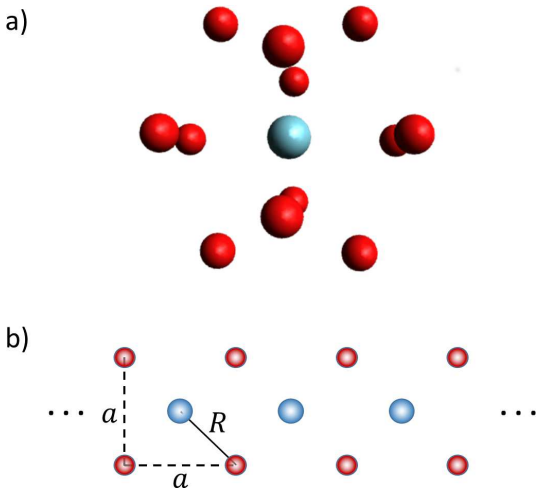

FIG. 3. a) $ArNe_{12}$ cluster of icosahedral symmetry. The drawing is by courtesy of E. Fasshauer. b) A planar lattice of four A atoms surrounding each B atom. The lattice is perpendicular to the polarization direction of the cavity and the lattice constant is a.

We searched for the maximal rate by rotating the cluster (rotation around Z does not change the rate) and found that rotating around the X-axis by 45° gives rise to $\Gamma = 0.3\,\Gamma_\pi$ and the transition dipole $\vec{D}_B$ points parallel to the Y-axis.

Finally, we address the issue of having more neighbors B. Since this is a whole subject by itself, we concentrate on one example which shows how to compute the ICD rate and demonstrates a particular impact of the cavity on ICD. Consider the lattice with lattice

constant a in the plane perpendicular to the polarization direction shown in Fig. 3b, where each B is surrounded by four equivalent A atoms. To be able to employ the equations derived above for a single B, we assign the index k to B and note that one can compute all required quantities for each B_k separately and obtain the partial rate Γ_k. For that purpose, R_i becomes the distance R_{ik} between B_k and A_i, γ_i becomes γ_{ik}, and so on. The total rate is then $\Gamma = \sum_{k=1}^{M} \Gamma_k$, where M is the number of B atoms. In the absence of cavity, a single atom A is excited and its decay rate due to its two nearest neighbors at distance $a/\sqrt{2}$ is $2\Gamma_\pi$. The next pair of neighbors are at distance $a\sqrt{(5/2)}$ and contribute $2\Gamma_\pi/5^3$ to the rate and the next pair $2\Gamma_\pi/13^3$. Adding the whole series shows that compared to considering only the next neighbors, the total impact of all other neighbors leads to a minor enhancement of 8.5×10^{-3} % which is rather negligible.

Now we consider the presence of the cavity and being in the XY-plane, we resort to Eq. (11) which gives the rate for a single B_k and where R_i is replaced by R_{ik}. To make contact with the cavity-free case, $R = a/\sqrt{2}$. Accordingly, B_k has four nearest neighbors which, if the other A atoms are not considered, gives rise to $\Gamma_k = \Gamma_\pi 4^2/(2N)$ and, for a long lattice, where $M = N/2$ and all B atoms have the same rate, $\Gamma = 4\Gamma_\pi$ which is twice as much as without the cavity. What about including farther away neighbors in the cavity? Following Eq. (11) leads to the series $\Gamma_k = \Gamma_\pi/(2N)[4 + 4(1/5)^{3/2} + 4(1/13)^{3/2} + ...]^2$, which after multiplication with $N/2$ gives the total rate $\Gamma = 5\Gamma_\pi$. We see that the impact of more remote neighbors is much more important in cavity than in its absence.

Due to the entanglement of the atoms A of an ensemble interacting with quantum light, the ICD process takes on very different features from classical ICD. One finds high sensitivity to the arrangement of the atoms and also to their orientation with respect to the polarization direction of the light, as well as to the position of the impurity B. Also, in cavity the impact of more remote atoms and the related inclusion of farther neighbors can be substantially more important. Interestingly, symmetric arrangements like an endohedral icosahedrons can become ICD inactive. This calls for studies of clusters. Here, antisymmetric vibrational modes can cause ICD activity and the impact of interactions between the atoms has to be investigated. This all can make the field of clusters in cavity fruitful. It should be mentioned that not only the ICD rate is of relevance, but also the fact that ICD electrons are emitted and their energy and angular distribution are of relevance. As we have seen for the tilted ring, even the direction of the transition dipole varies strongly with the tilt angle.

Of course, one can expect similar effects for molecules. However, nuclear dynamics makes molecule more complicated and as discussed in the introduction, molecules are more affected by the cavity since, e.g., light-induced conical intersections are created and such modifications must be included into the description of their dynamics. It has been recently shown that vibrational ICD [60] is efficient, where the excess vibrational energy of a molecule can be utilized to ionize a neighbor (e.g., anion). This reduces the involved energy substantially and enlarges the scope of ICD in cavity. The present study makes clear that one can expect related severe impact of quantum light also on other processes which follow transition-dipole transition-dipole interactions. Here, we mention Foerster resonance energy transfer [61–63] and resonant [64, 65] and non-resonant [66] vibrational energy transfer.

ACKNOWLEDGMENTS

The authors thank E. Fasshauer and K. Gokhberg for valuable contributions. Financial support by the European Research Council (ERC) (Advanced Investigator Grant No. 692657) is gratefully acknowledged

[1] L. S. Cederbaum, J. Zobeley, and F. Tarantelli, Phys. Rev. Lett. **79**, 4778 (1997).

[2] G. Öhrwall, M. Tchaplyguine, M. Lundwall, R. Feifel, H. Bergersen, T. Rander, A. Lindblad, J. Schulz, S. Peredkov, S. Barth, et al., Phys. Rev. Lett. **93**, 173401 (2004).

[3] A. I. Kuleff and L. S. Cederbaum, Phys. Rev. Lett. **98**, 083201 (2007).

[4] T. Jahnke, J. Phys. B **48**, 082001 (2015).

[5] T. Jahnke, H. Sann, T. Havermeier, K. Kreidi, C. Stuck, M. Meckel, M. Schffler, N. Neumann, R. Wallauer, S. Voss, et al., Nat. Phys. **6**, 139 (2010).

[6] M. Mucke, M. Braune, S. Barth, M. Förstel, T. Lischke, V. Ulrich, T. Arion, B. U., A. Bradshaw, and U. Hergenhahn, Nat. Phys. **6**, 143 (2010).

[7] S. Kopelke, Y.-C. Chiang, K. Gokhberg, and L. S. Cederbaum, J. Chem. Phys. **137**, 034302 (2012).

[8] G. Jabbari, K. Sadri, L. S. Cederbaum, and K. Gokhberg, J. Chem. Phys. **144**, 164307 (2016).

[9] N. Sisourat, N. V. Kryzhevoi, P. Kolorenc, S. Scheit, T. Jahnke, and L. S. Cederbaum, Nat.

Phys. **6**, 508511 (2010).

[10] T. Havermeier, T. Jahnke, K. Kreidi, R. Wallauer, S. Voss, M. Schöffler, S. Schössler, L. Foucar, N. Neumann, J. Titze, et al., Phys. Rev. Lett. **104**, 133401 (2010).

[11] A. Ben-Asher, A. Landau, L. S. Cederbaum, and N. Moiseyev, J. Phys. Chem. Lett. **11**, 6600 (2020).

[12] T. Goldzak, L. Gantz, I. Gilary, G. Bahir, and N. Moiseyev, Phys. Rev. B **91**, 165312 (2015).

[13] A. Bande, K. Gokhberg, and L. S. Cederbaum, J. Chem. Phys. **135**, 144112 (2011).

[14] I. Cherkes and N. Moiseyev, Phys. Rev. B **83**, 113303 (2011).

[15] F. M. Pont, A. Bande, and L. S. Cederbaum, Phys. Rev. B **88**, 241304 (2013).

[16] R. W. Howell, Int. J. Radiat. Biol. **84**, 959975 (2008).

[17] S. D. Stoychev, A. I. Kuleff, and L. S. Cederbaum, J. Am. Chem. Soc. **133**, 6817 (2011).

[18] U. Hergenhahn, Int. J. Radiat. Biol. **88**, 871 (2012).

[19] K. Gokhberg, P. Kolorenc, A. I. Kuleff, and L. S. Cederbaum, Nature **505**, 661 (2014).

[20] F. Trinter, M. S. Schöffler, H.-K. Kim, F. P. Sturm, K. Cole, N. Neumann, A. Vredenborg, J. Williams, I. Bocharova, R. Guillemin, et al., Nature **505**, 664 (2014).

[21] T. Jahnke, U. Hergenhahn, B. Winter, R. Dörner, U. Früling, P. V. Demekhin, K. Gokherg, L. S. Cederbaum, A. Ehresmann, A. Knie, et al., Chem. Rev. **120**, 11295 (2020).

[22] T. Schwartz, J. A. Hutchison, C. Genet, and T. W. Ebbesen, Phys. Rev. Lett. **106**, 196405 (2011).

[23] K. Stranius, M. Hertzog, and K. Börjesson, Nat. Commun. **9**, 2273 (2018).

[24] T. W. Ebbesen, Acc. Chem. Res. **49**, 2403 (2016).

[25] M. Kowalewski and S. Mukamel, Proc. Natl. Acad. Sci. **114**, 3278 (2017).

[26] J. Feist, J. Galego, and F. J. Garcia-Vidal, ACS Photonics **5**, 205 (2018).

[27] A. Thomas, L. Lethuillier-Karl, K. Nagarajan, R. Vergauwe, J. George, T. Chervy, A. Shalabney, E. Devaux, C. Genet, J. Moran, et al., Science **363**, 615 (2019).

[28] F. Herrera and F. C. Spano, Phys. Rev. Lett. **116**, 238301 (2016).

[29] A. Semenov and A. Nitzan, J. Chem. Phys. **150**, 174122 (2019).

[30] C. Schäfer, M. Ruggenthaler, and A. Rubio, Proc. Natl. Acad. Sci. **116**, 4883 (2019).

[31] A. Mandal, T. D. Krauss, and P. Huo, J. Phys. Chem. B **124**, 6321 (2020).

[32] M. Du, L. A. Martinez-Martinez, R. F. Ribeiro, Z. Hu, V. M. Menon, and J. Yuen-Zhou, Chem. Sci. **9**, 6659 (2018).

[33] M. Kowalewski, K. Bennett, and S. Mukamel, J. Chem. Phys. **144**, 054309 (2016).

[34] K. Bennett, M. Kowalewski, and S. Mukamel, Faraday Discuss. **194**, 259 (2016).

[35] N. Moiseyev, M. Sindelka, and L. S. Cederbaum, J. Phys. B **41**, 221001 (2008).

[36] G. J. Halász, A. Vibók, M. Sindelka, N. Moiseyev, and L. S. Cederbaum, J. Phys. B **44**, 175102 (2011).

[37] G. J. Halász, A. Vibók, and L. S. Cederbaum, J. Phys. Chem. Lett. **6**, 348354 (2015).

[38] T. Szidarovszky, G. J. Halasz, A. G. Csaszar, L. S. Cederbaum, and A. Vibok, J. Phys. Chem. Lett. **9**, 62156223 (2018).

[39] A. Csehi, M. Kowalewski, G. J. Halasz, and A. Vibok, New J. Phys. **21**, 093040 (2019).

[40] B. Gu and S. Mukamel, Chem. Sci. **11**, 1290 (2020).

[41] C. Fabri, G. J. Halasz, L. S. Cederbaum, and A. Vibok, Chem. Sci. ,DOI: 10.1039/d0sc05164k (2020).

[42] O. Vendrell, Phys. Rev. Lett. **121**, 253001 (2018).

[43] C. Cohen Tannoudji, J. Dupont-Roc, and G. Grynberg, *Atom-Photon Interactions: Basic Processes and Applications* (Wiley, Weinheim, 2004).

[44] C. Müller, M. A. Macovei, and A. B. Voitkiv, Phys. Rev. A **84**, 055401 (2011).

[45] F. H. M. Faisal, *Theory of Multiphoton Processes* (Springer, New-York, 1987).

[46] J. Galego, F. J. Garcia-Vidal, and J. Feist, Phys. Rev. X **5**, 041022 (2015).

[47] O. Vendrell, Chem. Phys. **509**, 55 (2018).

[48] J. H. Wilkinson, *The Algebraic Eigenvalue Problem* (Clarendon Press, Oxford, 1965).

[49] O. Walter, L. S. Cederbaum, and J. Schirmer, J. Math. Phys. (N.Y.) **25**, 729 (1984).

[50] D. OLeary and G. Stewart, J. Comput. Phys. **90**, 497 (1990).

[51] K. Gokhberg, N. V. Kryzhevoi, P. Kolorenc, and L. S. Cederbaum, Phys. Rev. A **81**, 013417 (2010).

[52] S. Kopelke, K. Gokhberg, V. Averbukh, F. Tarantelli, and L. S. Cederbaum, J. Chem. Phys. **134**, 094107 (2011).

[53] A. M. Flusberg, Phys. Rev. A **24**, 3080 (1981).

[54] M. Mehring and J. S. Waugh, Phys. Rev. B **5**, 3459 (1972).

[55] A. Mhamdi, J. Rist, D. Aslitürk, M. Weller, N. Melzer, D. Trabert, M. Kircher, I. Vela-Pérez, J. Siebert, S. Eckart, et al., Phys. Rev. Lett. **121**, 243002 (2018).

[56] A. Mhamdi, F. Trinter, C. Rauch, M. Weller, J. Rist, M. Waitz, J. Siebert, D. Metz, C. Janke,

G. Kastirke, et al., Phys. Rev. A **97**, 053407 (2018).

[57] G. Scoles, ed., *The Chemical Physics of Atomic and Molecular Clusters* (North Holland, Amsterdam, 1990).

[58] R. Viskup, *Femtosecond Laser Pulse Interaction with Rare Gas Clusters* (Lambert Acad. Publ., Berlin, 2011).

[59] A. K. Rappe, C. J. Casewit, K. S. Colwell, W. A. Goddard, and W. M. Skiff, J. Am. Chem. Soc. **114**, 10024 (1992).

[60] L. S. Cederbaum, Phys. Rev. Lett. **121**, 223001 (2018).

[61] T. Förster, Ann. Phys. (Berlin) **437**, 55 (1948).

[62] T. Renger, V. May, and O. Kühn, Phys. Rep. **343**, 137 (2001).

[63] G. D. Scholes, G. R. Fleming, A. Olaya-Castro, and R. van Grondelle, Nat. Chem. **3**, 763774 (2011).

[64] S. Woutersen and H. J. Bakker, Nature **402**, 507509 (1999).

[65] H. Chen, X. Wen, X. Guo, and J. Zheng, Phys. Chem, Chem. Phys. **16**, 13995 (2014).

[66] L. S. Cederbaum, Mol. Phys. **117**, 19501955 (2019).